Marine Geology 254 (2008) 121–128

Contents lists available at ScienceDirect

Marine Geology

journal homepage: www.elsevier.com/locate/margeo

Wave climate, sediment supply and the depth of the sand–mud transition: A global survey

Douglas A. George [a,*], Paul S. Hill [b]

[a] United States Geological Survey, Santa Cruz, California, USA
[b] Department of Oceanography, Dalhousie University, Halifax, Nova Scotia, Canada

ARTICLE INFO

Article history:
Received 6 September 2007
Received in revised form 30 April 2008
Accepted 11 May 2008

Keywords:
Sand–mud transition
Continental shelf
Sedimentation
Mudline
Wave energy
Bed shear stress

ABSTRACT

The influences of wave climate and sediment supply on the depths of sand–mud transitions (h_{SMT}) are investigated. Depths of sand–mud transitions (SMT) are based on published granulometric data from surface samples gathered from 14 sites in different wave-dominated coastal environments with fluvial input, including high energy (Columbia, Eel, Russian, San Lorenzo, Copper, and Nepean rivers), moderate energy (Ebro, Nile, Santa Clara, Tseng-wen and Kao-ping rivers), and low energy (Po, Pescara and Tronto rivers) regimes. Geometric mean diameter (GMD) and mud percent are compiled from samples along shore-normal transects, and significant correlation is found between these two textural descriptors. Nominally, the SMT is defined as the transition from GMD >63 μm to <63 μm. The correlation between mud percent and GMD permits an alternative, complementary definition of the SMT as the transition from <25% mud to >25% mud. This dual definition is applied to the 14 systems, and h_{SMT} is tabulated for each system. Correlation is found between h_{SMT} and the depth at which wave-induced bottom shear stress equals the critical erosion shear stress of the largest mud particles and also between h_{SMT} and significant wave height. Lack of correlation between h_{SMT} and sediment load of nearby rivers indicates either that the influence of sediment supply on depth of the sand–mud transition is small or is not adequately represented in this study. Shelf width and slope do not correlate with residuals from a formalized linear relationship between h_{SMT} and significant wave height. The relationship between h_{SMT} and wave climate is useful for calibration of numerical models of erosion and deposition in wave-dominated coastal environments, for prediction of seabed properties in remote or inaccessible areas, and for reconstruction of paleodepth based on facies changes from sand to mud in ancient rocks.

1. Introduction

The sand–mud transition (SMT) is a boundary on the seafloor where the dominant grain size changes from sand to silts and clays, known collectively as "mud" (McCave, 1972). A sand–mud transition nominally is defined as the place on the seabed where mean grain size falls below 63 μm. Alternatively, it can be identified as the region of the seafloor where the mass percentage of grains with diameters <63 μm in the sediment increases rapidly. This boundary is also called the "mudline" (Stanley et al., 1983), although for this study the term SMT is used exclusively.

The SMT is important because biological, physical, geological and chemical processes are substantially different on either side of this boundary. Sands and muds host different benthic communities (Snelgrove and Butman, 1994), have different acoustic properties (Goff et al., 1999), and, carry different concentrations of heavy metals and biogenic particles (e.g., Milligan and Loring, 1997; Schiff, 2000; George et al., 2007). From a geological perspective, the transition from sand to mud represents a basic lithologic facies change that has been mapped in the rock record to infer depositional environments (Clifton, 1986; Dunbar and Barrett, 2005).

The sand–mud transition occurs in different water depths on different margins. The factors that determine the depth of the sand–mud transition are debatable. In the most comprehensive assessment, Stanley et al. (1983) argue that the depth of the SMT on a given margin depends primarily on the energy levels of the physical forcing on a margin, with deeper SMTs occurring in more energetic environments. They also argue that many secondary parameters may influence the depth of this boundary, including sediment supply, shelf width, shelf break morphology, and sediment stability. Of these, proximity to fluvial sediment input has been identified as a particularly important factor (Palanques and Drake, 1990; Meadows et al., 2002; Hill et al., 2007).

McCave (1972) proposed that mud accumulation on the seafloor occurs when depositional flux exceeds erosional flux. This simple argument indicates that on a wave-dominated coast, both wave climate and sediment supply influence the depth of the SMT. More specifically, depositional flux is large when near-bed suspended-sediment concentration is large and bed shear stress is low (e.g.,

* Corresponding author. 400 Natural Bridges Dr., Santa Cruz, CA, USA, 95060. Tel.: +1 831 427 4759; fax: +1 831 427 4748.
E-mail address: doug.george@gmail.com (D.A. George).

0025-3227/$ – see front matter © 2008 Published by Elsevier B.V.
doi:10.1016/j.margeo.2008.05.005

Milligan et al., 2007). Erosional flux depends on both the boundary shear stress exerted by waves and currents, and on the physical properties of the seabed, such as cohesion and grain size (Wiberg et al., 1994; Sanford and Maa, 2001).

Recently, Dunbar and Barrett (2005) addressed the relationship between energy and depth of the SMT. Specifically, they examined how predicted cross-margin distribution of boundary shear stress affected the depth of the SMT in three coastal settings (low energy — Wellington Harbor, New Zealand; moderate energy — Manawatu coast, New Zealand; high energy — Monterey Bay, USA). They operated under a few simplifying assumptions. Shear stress was assumed to be entirely due to waves, and the wave climate was characterized simply with average significant wave height and dominant wave period. They assumed that no mud could deposit at shear stresses greater than the critical erosion shear stress of a 63 μm silt grain, and they set the value of this critical erosion shear stress as τ_c=0.08 Pa. Using wave climatology for their three margins, Dunbar and Barrett (2005) calculated the depth at which the wave-induced shear stress fell below 0.08. The calculated depths compared reasonably well with the observed depths of the SMTs.

The simple rule for determining depth of the SMT proposed by Dunbar and Barrett (2005) would be useful to a variety of fields. Given that the rule was assessed on only three margins, however, its broad applicability to wave-dominated margins and its predictive power are uncertain. The overall goal of this paper is to examine, with data from as many different wave-dominated margins as possible, the strength of correlation between observed depth of the SMT and the depth where wave-induced shear stress equals 0.08 Pa. In addition, correlations between depth of the SMT and other environmental variables are examined, namely river sediment discharge, shelf width, and shelf gradient. The ultimate goal of this research is to generate a correlative model that ties one or more of the environmental variables to the SMT depth. Such a model could be useful to assess sediment deposition in numerical models (e.g., Pratson et al., 2007), to estimate the likely h_{SMT} in regions where sedimentological data are unavailable, or to reconstruct paleodepths at facies boundaries in the rock record (e.g. Dunbar and Barrett, 2005).

2. Materials and methods

2.1. Data compilation

Sediment dispersal systems were chosen to investigate the SMT based on three criteria: 1) a clearly identifiable SMT; 2) an estimate for sediment load from a nearby river (Q_s, t/yr); and, 3) a well-described wave climate. Wave data are routinely available on many coasts, and estimates for sediment load are available for well monitored or extensively studied river systems. Relevant wave climate parameters were average significant wave height ($H_{1/3}$, m) and dominant wave period (T_{dom}, s). Details for each parameter follow.

Sediment textural data representing a diverse set of environments were compiled for 14 SMTs from published scientific literature and unpublished records acquired directly from researchers (Table 1; Fig. 1; see Online Supplement for site maps). See the appropriate reference for the quality control on published data. Data acquired from the goSEABED database for the Nepean were quality checked by the data supplier (Jenkins et al., 2003). The laboratory procedures of the unpublished records were scrutinized to ensure the analysis conformed to standard analysis techniques. The Santa Clara sediment was analyzed at the U.S.G.S. Coastal and Marine Geology sedimentology laboratories in Menlo Park, CA, while the Eel sediment was analyzed at the Bedford Institute of Oceanography Particle Dynamics Laboratory in Dartmouth, Nova Scotia, Canada.

Table 1
Environmental conditions and available data for 14 SMTs

SMT system	Number of cross-shelf transects	Total number of sediment samples	Bed sediment source	Sediment load (Q_s, t/yr)	Q_s source	Average significant wave height ($H_{1/3}$, m)	Dominant wave period (T_{dom}, s)	Wave data source
High energy								
Columbia, USA	3	22	Reid et al. (2006)	12.0e6	Milliman and Syvitski (1992)	2.3	10.7	NDBC[a] Buoy #46029
Eel, USA	1	12	Milligan (unpublished data)	24.0e6	Milliman and Syvitski (1992)	2.4	11.1	NDBC[a] Buoy #46022
Russian, USA	5	28	Demirpolat (1991)	4.0e6	Milliman and Syvitski, (1992)	2.3	11.2	NDBC[a] Buoy #46013
San Lorenzo, USA	2	11	Edwards (2002)	6.6e6	Milliman and Syvitski, (1992)	2.2	7.4	NDBC[a] Buoy #46042
Nepean, Australia	2	12	Jenkins et al. (2003)	1.5e6	Milliman et al, 1995	1.6	8.0	Short and Trenaman, 1992
Copper, USA	2	11	Jenkins et al. (2003)	70.0e6	Milliman and Syvitski, (1992)	2.4	9.9	NDBC[a] Buoy #46082
Moderate energy								
Ebro, Spain	3	21	Palanques and Drake (1990)	18.0e6[b]	Milliman and Syvitski (1992)	0.8	5.9	Tarragona buoy
Nile, Egypt	3	17	Frihy and Gamai (1991)	120.0e6[b]	Milliman and Syvitski (1992)	1.2	5.6	Frihy, unpublished
Tseng-wen, Taiwan	17	194	Liu et al. (2003)	31.0e6	Milliman and Syvitski (1992)	0.5	5.4	Liu et al. (2003)
Kao-ping, Taiwan	19	143	Liu et al. (2002)	36.0e6	Milliman and Syvitski (1992)	0.5	5.4	Liu et al. (2002)
Santa Clara, USA	1	6	Warrick (unpublished data)	6.0e6	Milliman and Syvitski (1992)	1.3	6.6	NDBC[a] Buoy #46053
Low energy								
Tronto, Italy	5	26	George et al. (2007)	1.1e6	Milliman and Syvitski (1992)	0.7	3.2	Ortona buoy
Pescara, Italy	16	75	George et al. (2007)	0.9e6	Milliman and Syvitski (1992)	0.7	3.2	Ortona buoy
Po, Italy	1	5	Fox et al. (2004)	17.0e6	Milliman and Syvitski (1992)	0.7	3.2	Fain et al. (2007)

[a] NDBC (National Data Buoy Center).
[b] Historical sediment load. See Appendix for site maps.

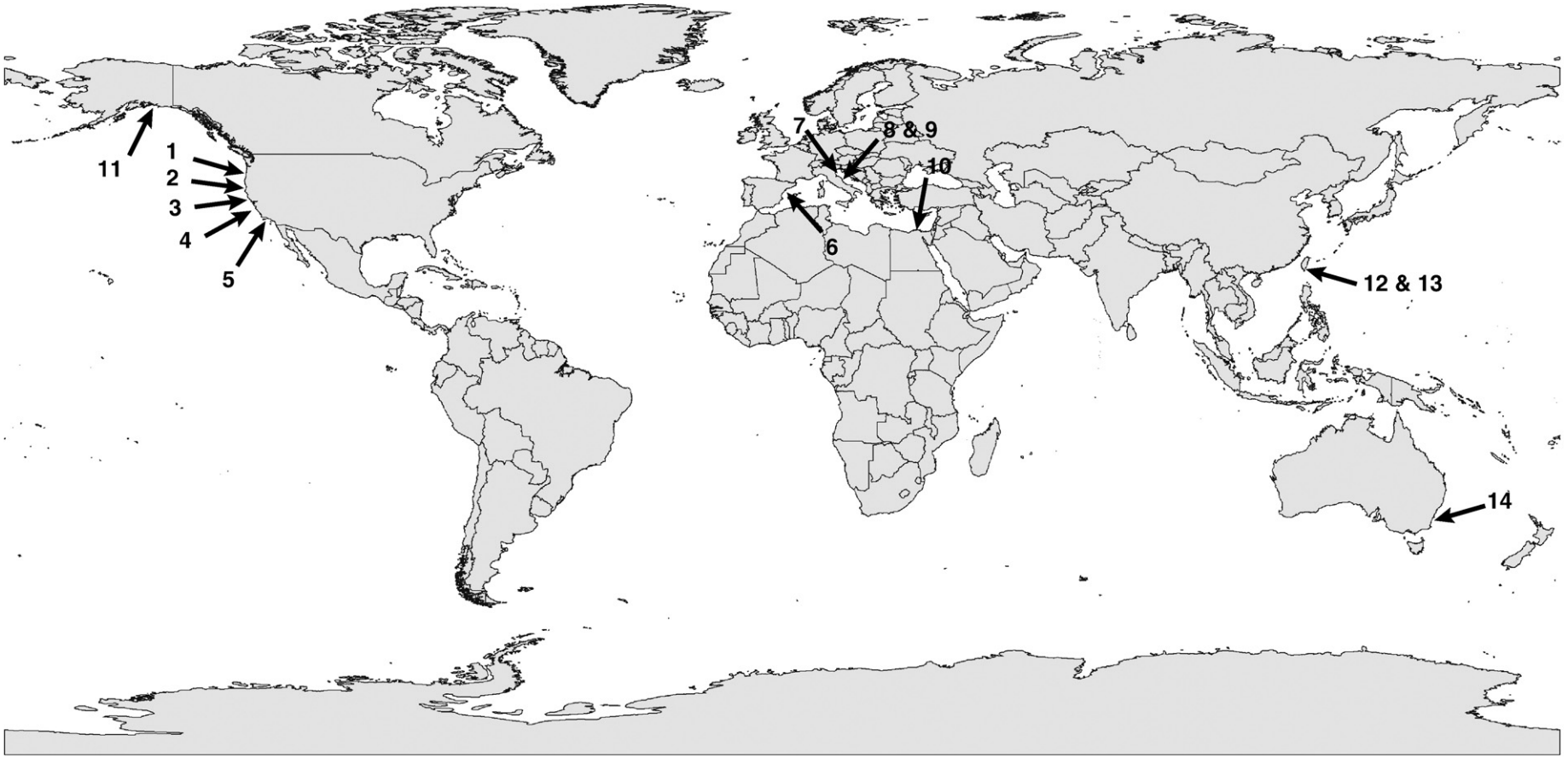

Fig. 1. Locations of the 14 SMTs included in this study: 1) Columbia, USA; 2) Eel, USA; 3) Russian, USA; 4) San Lorenzo, USA; 5) Santa Clara, USA; 6) Ebro, Spain; 7) Po, Italy; 8) Tronto, Italy; 9) Pescara, Italy; 10) Nile, Egypt; 11) Copper, USA; 12) Tseng-wen, Taiwan; 13) Kao-ping, Taiwan; and 14) Nepean, Australia. See Appendix for site maps.

Mean grain size is not always available in sedimentological data sets so, by selecting only this one sediment descriptor, the amount of data available to explore controls on the depth of the SMT is limited. In this study, correlation is sought between mean grain size at the SMT and percent mud at the same point. If the correlation is robust, then either parameter could be used to identify an SMT. To develop such a correlation, cross-shelf transects of sediment samples that provide geometric mean diameter (GMD) and mud percent at discrete positions were identified for 11 systems. For the Tseng-wen and Kao-ping, no grain size data for the samples were available and conversely, no mud percent information was available for the Po.

The length of sediment load records varies widely around the world. As most of the sediment load values were selected from Milliman and Syvitski (1992), their methods of averaging were assumed to be satisfactory for the purposes of this study. Deriving an estimate for sediment load over long time scales from a river adjacent to one of the selected SMTs is problematic when the river has been significantly dammed in recent decades, as have, for example, the Nile or Ebro. Modern data represent modern fluvial conditions, but SMTs may be the product of longer term patterns of accumulation (Crockett and Nittrouer, 2004; George et al., 2007). Therefore, historical estimates of discharge were used for heavily modified rivers.

The methods used to report wave climates varied widely. Most of the records are from buoy observations with average significant wave height and dominant wave period reported for the duration of the record. While some records are decades long, such as at the Eel or Columbia River margins, others are much shorter (e.g., three years of data for the Tronto and Pescara). The average significant wave height for the Po was extracted from data collected during a 9-month tripod deployment but no data for wave period were available (Fain et al., 2007). In addition to the length of a record, the depth where the wave climate is described also affected the averaged results due to shoaling effects. For example, data from the Monterey Bay buoy (NDBC#46042) come from 2115 m while those from the Santa Barbara Channel (NDBC#46053) were collected in 417 m and the Po tripod were from 12 m. The depth disparities among the collection sites are an unquantified source of error in this study.

2.2. Defining the sand–mud transition

The relationship between sediment grain size and classification was explored to generate multiple, mutually consistent definitions of the SMT. The correlation between percent mud and GMD is strong ($R^2=0.67$, $p<0.01$). Most of the GMD samples pass from sand to mud in size between 20 and 30% mud (Fig. 2). Based on these data, a standard definition of the SMT is proposed as the demarcation where the GMD fines from >63 μm to <63 μm, or percent mud changes from <25% to >25%. If both parameters were available, as was the case for 11 systems, then the default parameter was the one based on GMD. The definition was applied to the samples along each transect, and the transition depth was recorded (Table 2). In systems with multiple transects (see Table 1), a mean transition depth was calculated. The Po SMT, which lacked percent mud data, was determined on GMD only while the Tseng-wen and Kao-ping SMTs were determined based on percent mud data.

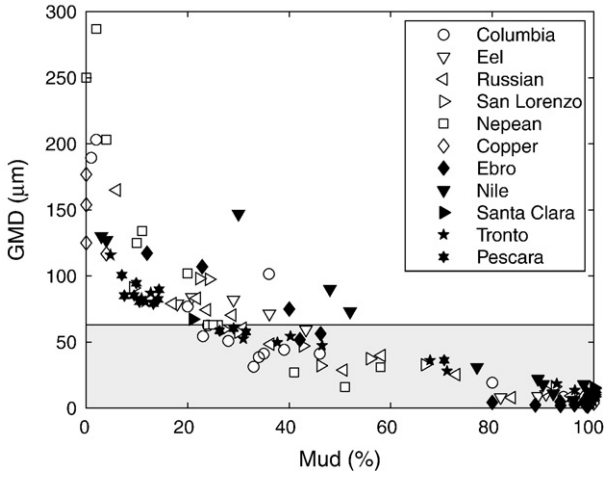

Fig. 2. Percent mud and geometric mean diameter (GMD) for all cross-shelf transect stations available from 11 systems. The gray zone represents the mud classification at GMD <63 μm. The majority of the data crosses into the mud category when percent mud is 20–30% mud.

Table 2
SMT depth, shelf width and slope for 14 SMTs

	SMT depth (h_{SMT}, m)	Shelf width* (km)	Slope at SMT (m/km)
High energy			
Columbia, USA	50	70	6.75
Eel, USA	55	20	4.25
Russian, USA	50	40	8.25
San Lorenzo, USA	40	17	5.68
Nepean, Australia	60	50	5.17
Copper, USA	50	50	2.00
Moderate energy			
Ebro, Spain	30	95	1.44
Nile, Egypt	20	80	0.91
Tseng-wen, Taiwan	11	[a]	1.00
Kao-ping, Taiwan	25	[a]	3.22
Santa Clara, USA	30	50	6.71
Low energy			
Tronto, Italy	15	[a]	2.77
Pescara, Italy	20	[a]	2.74
Po, Italy	6	[a]	3.60

* — to 100 m isobath; a — not definable.

2.3. Secondary parameters

Stanley et al. (1983) suggest a secondary dependence on shelf width for the SMT. Shelf width normal to a river mouth was estimated for nine of the 14 systems at the 100 m isobath where a shelf break was definable (Table 2). The shelf gradient, or bed slope, at the SMT was also calculated after h_{SMT} was determined for each system.

2.4. Shear stresses across margins

Following the example of Dunbar and Barrett (2005), cross-shelf profiles of wave-induced shear stress (τ_w) were calculated for the 14 systems investigated in this study. The profiles, as well as three calculated from the Dunbar and Barrett (2005) study (Petone Beach, Peka Peka and Monterey Bay), estimate the depths at which stress falls below 0.08 Pa (Fig. 3). At this stress, silt and clay particles are able to deposit, allowing transition to a mud-dominated seabed sediment (Dunbar and Barrett, 2005). Using the energy regimes defined in the Dunbar and Barrett analysis, the profiles group according to the energy level of the environment with the higher energy systems (open symbols) corresponding to a deeper depth where $\tau_w<0.08$ Pa and the lower energy systems (gray symbols) showing shallower depths. The depths where $\tau_w=0.08$ Pa were tallied for comparison to the observed depths of sand–mud transitions on the various margins.

3. Results

3.1. Depth of SMT, shear stress and wave heights

The depths where $\tau_w=0.08$ Pa were plotted against h_{SMT} for the 17 systems (14 from this study, three from Dunbar and Barrett, 2005), producing a moderately strong correlation of $R^2=0.69$ ($p<0.01$) (Fig. 4). As energy increases, deeper h_{SMT} values are observed with the exposed

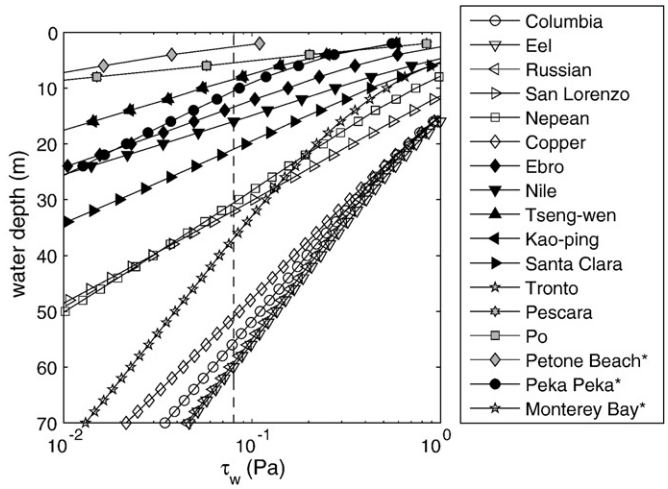

Fig. 3. Cross-shelf profiles of wave-induced shear stress (τ_w) calculated for the 14 systems compiled for this study and three from Dunbar and Barrett (2005) (*). The dashed line indicates τ_w=0.08 Pa. Using the energy regimes defined in the Dunbar and Barrett analysis, the profiles group according to the energy level of the environment with the higher energy systems (open symbols) corresponding to a deeper depth where τ_w=0.08 Pa and the lower energy systems (gray symbols) showing shallower depths.

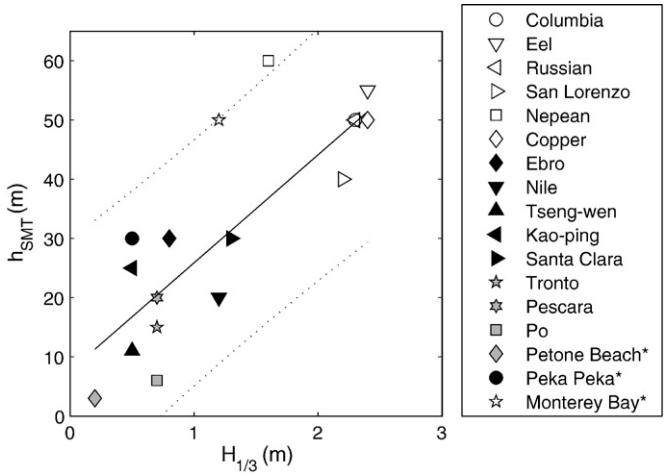

Fig. 5. Average significant wave height ($H_{1/3}$, m) and the sand–mud transition depth (h_{SMT}, m) for the 14 systems compiled for this study and three from Dunbar and Barrett (2005) (*). The colors of the symbols correspond to the energy level with higher (open), moderate (black) and lower (gray) definitions following Dunbar and Barrett (2005). Deeper SMTs are observed as wave height increases, and this correlation is significant with R^2=0.84 (p<0.01) when the Nepean is excluded. Dashed lines indicate the 95% prediction interval for Eq. (2) for the range of significant wave heights displayed.

systems of the northeastern Pacific (Eel, Russian and Columbia) showing the deepest h_{SMT}. Ninety-five percent prediction intervals show that that using the depth where τ_w=0.08 Pa to predict h_{SMT} constrains h_{SMT} within a depth range of 40 m. To improve the relationship, the Nepean, which does not follow the trend observed for the other 16 systems, was considered an outlier and excluded, yielding

$$h_{SMT} = (0.74\pm0.36)h_{\tau(0.08)} + (12.21\pm11.78) \quad (1)$$

where $h_{\tau(0.08)}$ is the depth where τ_w=0.08 (m) and with 95% confidence intervals. The correlation strengthens considerably (R^2=0.84; p<0.01), and the prediction intervals tighten to approximately 30 m. Residuals for all of the systems were calculated for further investigation against the secondary parameters.

Dunbar and Barrett (2005) use wave height and wave period to predict $h_{\tau(0.08)}$. Because these two parameters typically co-vary, a simpler predictor of h_{SMT} may be significant wave height. The correlation between $H_{1/3}$ and h_{SMT} is significant (R^2=0.72; p<0.01). Shallowest SMTs are observed at the smallest $H_{1/3}$ and the deepest transitions (e.g., Eel at 55 m, Columbia and Russian at 50 m) occur when $H_{1/3}$ >2 m (Fig. 5). Although a gap in the data exists in the region of $H_{1/3}$ of 1.5–2 m and h_{SMT} of 30–40 m, a trend of deeper h_{SMT} with increasing average significant wave heights is evident. The Nepean again does not follow the trend in the other systems, with a moderate $H_{1/3}$ (1.59 m) and deep h_{SMT} (60 m). When excluded, the correlation improves (R^2=0.84; p<0.001). The relationship without the Nepean can be quantified with a simple linear relationship,

$$h_{SMT} = (18.5\pm10.8)H_{1/3} + (5.2\pm17.2) \quad (2)$$

where $H_{1/3}$ is the significant wave height (m) and with 95% confidence intervals.

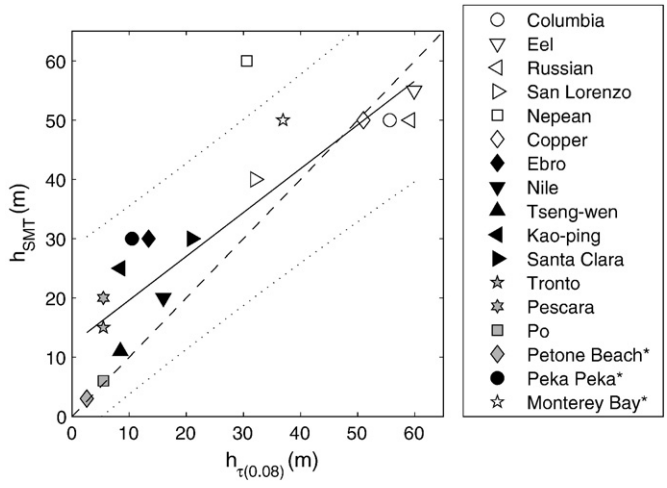

Fig. 4. Depth where τ=0.08 Pa ($h_{\tau(0.08)}$, m) and the sand–mud transition depth (h_{SMT}, m) for the 14 systems compiled for this study and three from Dunbar and Barrett (2005) (*). The colors of the symbols correspond to the energy level with higher (open), moderate (black) and lower (gray) definitions following Dunbar and Barrett (2005). The dashed line is a 1:1 relationship and the dotted lines are the 95% prediction intervals around the regression line, described as Eq. (1). When the Nepean is excluded, the correlation is significant (R^2=0.84; p<0.01), and the prediction intervals tighten to approximately 30 m.

3.2. Secondary parameters

Sediment loads for the 14 systems range widely from 0.9×10^6 t/yr (Pescara) to 120×10^6 t/yr (Nile) (Table 2). The wave climate of the coast does not appear associated with Q_s. Shelf widths, where definable, and the slope at h_{SMT} are also not correlated with wave climate, although no shelf widths were determined for the low energy category.

No significant correlation was observed between sediment load and h_{SMT} in a direct comparison for the 14 systems being examined (R^2=0.06, p=0.41). Because sediment load had been identified as a probable contributor to the SMT, Q_s and the residuals from the relationship determined for h_{SMT} and τ_w were compared but no discernable patterns emerged (Fig. 6A). Likewise, the residuals were compared against shelf width and slope (Fig. 6B and C, respectively) with the same result of no relationship.

4. Discussion

4.1. Defining the sand–mud transition

The multi-parameter standard definition of the SMT proposed above is possible because of the observed relationship between GMD and percent mud. The dual nature of the definition allowed the inclusion of systems lacking one or the other of the parameters (Po — GMD only;

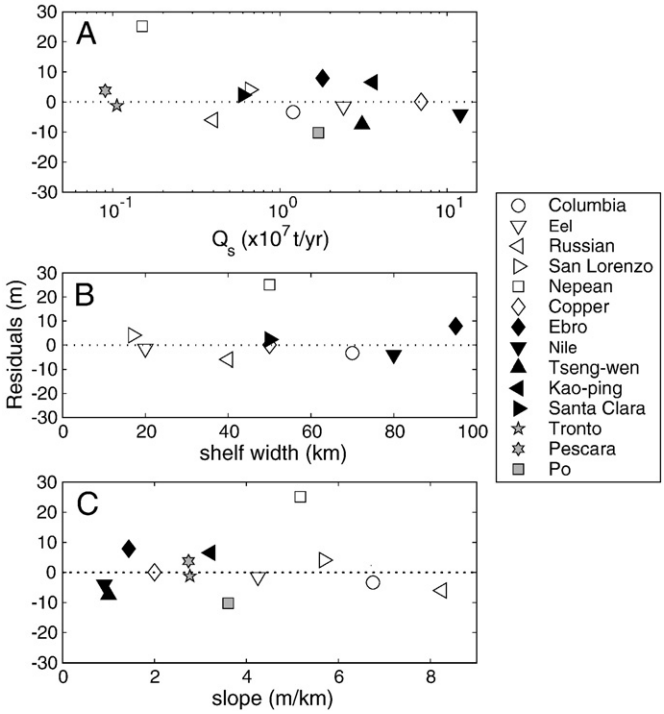

Fig. 6. Residuals from Eq. (1) for the 14 systems and A) sediment load from a nearby river, B) shelf width, and C) slope. The colors of the symbols correspond to the energy level with higher (open), moderate (black) and lower (gray) definitions following Dunbar and Barrett (2005). All three parameters have insignificant relationships with the residuals (p=0.40, 0.23, 0.31, respectively). See Table 2 for shelf width and slope data.

Tseng-wen and Kao-ping — sediment classification only). This definition may be applied now to coastal sedimentary maps, where facies are described in terms of mud content (e.g., Eittreim et al., 2000).

4.2. Examination of the shear stress and significant wave height models

Dunbar and Barrett (2005) proposed shear stress as a predictor of the h_{SMT}, but they did not investigate the broad applicability because only three systems were analyzed. To expand the Dunbar and Barrett (2005) approach and to remain consistent with their model assumption, only wave-dominated coasts were selected. By calculating $h_{\tau(0.08)}$ from $H_{1/3}$ and wave period, this study combined the three Dunbar and Barrett systems and the 14 systems identified from around the world. The significant correlation indicates that shear stress (and by extension, $H_{1/3}$) accounts for most of the variability in h_{SMT}, an observation that has been suggested (Stanley et al., 1983) but not quantified.

The slope of Eq. (1) is substantially different from a 1:1 line, indicating the equation is not accounting for other processes accurately (Fig. 4). For example, observed h_{SMT} are deeper than predicted for the shallower waters, but in deep water predicted and observed h_{SMT} are closer in magnitude. Several factors may explain the difference between observations and predictions. First, currents may add to the stress in shallow water, which is not accounted for in the model. Shoaling transformations of waves may cause larger-than-predicted maximum stresses and the effect is more acute in shallow water depths (Thorton and Guza, 1989; Herbers et al., 2003). The model uses simple linear wave theory and therefore may underpredict the depth of the shallower SMTs. Finally, storm wave parameters may be more appropriate than mean wave parameters for predicting h_{SMT}. Despite these shortcomings, Eq. (1) provides a direct connection between h_{SMT} and the deposition threshold proposed by Dunbar and Barrett. In practical terms, Eq. (2) may be a more useful relationship as $H_{1/3}$ is the only input required to estimate h_{SMT}, with the caveats for Eq. (1) extended to Eq. (2).

The strong correlation between significant wave height and the h_{SMT}, which supports the argument of Stanley et al. (1983), could be used to argue that all that is required to predict any h_{SMT} would be $H_{1/3}$. However, this first-order interpretation of the relationship is incorrect, as mud deposits are found in coastal areas that are not wave-dominated. For example, on the Australian continental shelf, Porter-Smith et al. (2004) classified the shelf by differentiating between wave- and tidal-dominated environments. They found that ~31% of the shelf was wave-only dominated, and ~41% of the shelf was tidal-only dominated, but the mud deposits in the tidal regions were more poorly sorted and finer grained. Further, wave climates contain strong seasonal patterns and intra-decadal cycles, such as El Nino-Southern Oscillation for the U.S. West Coast (Wingfield and Storlazzi, 2007). If $H_{1/3}$ is used exclusively, the wave climate should be divided into periods of different activity levels (quiescent times to extreme events) to produce a range of possible h_{SMT} on a given coastline. Although both Crockett and Nittrouer (2004) and George et al., (2007) showed that SMTs are relatively constant in time and space, some consideration should be given to the limitations of using Eq. (2). Nonetheless, the relationship explored in this current study suggests that, at least for the wave-dominated environments, significant wave height can explain the majority of the variance in h_{SMT}.

4.3. Secondary parameters

The lack of a direct relationship between river sediment load and h_{SMT} prompted examination of sediment load as a secondary parameter. However, no relationship between river sediment load and the residuals from Eq. (1) is evident for the 14 river systems. These results suggest either that sediment supply exerts little or no control on the depth of the SMT or that river sediment load does not adequately represent the effect of sediment supply. The effect of advection and diffusion in the littoral zone is ignored by assuming a nearby river is the only source of fine sediment. For the Tronto and Pescara, George et al. (2007) suggest that southerly currents on the western boundary of the Adriatic Sea contribute sediment to those SMTs. Similarly, the presence of a well-defined SMT along a region of the central California coast with small fluvial inputs indicates fine-grained sediment is accumulating from multiple distant sources (Storlazzi et al., 2007). The same phenomenon is observed in the East Indies (Milliman et al., 1999). Advection is also cited by Friedrichs and Wright (2004) for shaping equilibrium profiles on shelves near river mouths. A more robust and comprehensive approach may be needed to unravel the role of sediment supply in determining the depth of the SMT.

Stanley et al. (1983) suggest shelf width as a secondary parameter for the position of the sand–mud transition. The residuals from Eq. (1) for the 14 systems were examined against shelf width and slope and neither produced significant correlations with the residuals (p=0.23, 0.31, respectively). Additional comparisons of the residuals with distance of h_{SMT} from the shelfbreak (difference of the shelf width and distance from the shore to the h_{SMT}), and the position of h_{SMT} as a percentage of shelf width (quotient of the distance of h_{SMT} from the shelfbreak and the shelf width) also did not produce significant relationships (p=0.23, 0.98, respectively). The lack of any apparent relationships indicates that the suggested secondary parameters cannot enhance the efficacy of Eq. (1), and these variables are either poorly parameterized or unimportant for consideration of the controls on h_{SMT}.

4.4. Potential applications of Eq. (2)

The relationship between $H_{1/3}$ and h_{SMT} described in Eq. (2) provides an equation that can be utilized in several ways. For a wave-dominated coastline, Eq. (2) allows a reasonable estimation of h_{SMT} regardless of sediment supply or prior knowledge of the sediment distribution on the seafloor. High energy coastal environments have deeper SMTs compared to moderate to low energy ones. Eq. (2), with the associated 95% prediction intervals, would be useful in numerical modeling studies to assess predicted sediment dispersal patterns (e.g.,

Pratson et al., 2007). In particular, models could be evaluated in part on their ability to predict the depth of the SMT accurately. Output from Eq. (2) could be also employed in lieu of a sediment collection effort in regions where data acquisition is not possible for logistical or accessibility reasons. Another application of Eq. (2) is to reconstruct paleodepth based upon approximations of $H_{1/3}$ as Dunbar and Barrett (2005) did with their model and Clifton (1986) did for exposed deposits in Hungary and California. Significant wave height depends on wind speed, fetch, and duration, and estimates of these variables provide the necessary information to solve first for $H_{1/3}$ and then for h_{SMT}. Paleo-h_{SMT} could then be used in determining the depths of residence for fossilized flora and fauna or the depth of a lithified SMT observed in a stratigraphic record. Alternatively, if paleodepth of a sand–mud transition has been determined by flora or fauna (e.g., Naish and Kamp, 1997), Eq. (2) could be used to estimate paleo-$H_{1/3}$ for a region.

5. Conclusions

This study proposes a definition of the sand–mud transition (SMT) and investigates hypothesized controls on the depth of the SMT (h_{SMT}). Sediment data, wave climates, and nearby fluvial input were compiled for 14 SMTs on wave-dominated coasts to expand previous work (Dunbar and Barrett, 2005). The relationship between geometric mean diameter and mud percent was explored to produce a multi-parameter definition of the SMT as the demarcation from geometric mean diameter (GMD) >63 μm to <63 μm, or where percent mud grows larger than 25%. Correlation analysis shows that significant wave height has a strong relationship with h_{SMT} (R^2 = 0.84). The lack of any significant correlation between h_{SMT} and riverine sediment load suggests a more robust and comprehensive approach is necessary to incorporate sediment supply, possibly a combination of advective and diffusive sediment transport mechanisms. Correlations were not found for the suggested secondary parameters of shelf width and slope. The formalized relationship between h_{SMT} and $H_{1/3}$ provides a tool that might be useful in numerical modeling, sedimentology and paleo-oceanographic studies.

Acknowledgements

The data presented in this study were acquired by extremely generous researchers from around the world, including Jon Warrick (USGS), Tim Milligan (Bedford Institute of Oceanography, Canada), Omran Frihy (Coastal Research Institute, Egypt), James Liu (National Sun Yat-sen University, Taiwan), Chris Jenkins (University of Colorado, Boulder), Brian Edwards (USGS), Albert Palanques (Instituto de Ciencias del Mar, Spain), and Jane Reid (USGS). The manuscript benefited from the comments of Jon Warrick and Amy Draut and from the reviews of Alan Orpin, John Wells, and an anonymous reviewer. This work was supported by Homa J. Lee, USGS.

Appendix A. Supplementary data

Supplementary data associated with this article can be found, in the online version, at doi:10.1016/j.margeo.2008.05.005.

References

Clifton, H.E., 1986. Interpreting paleoenergy levels from sediment deposited on ancient wave dominated shelves. In: Knight, R.J., McLean, J.R. (Eds.), Shelf Sands and Sandstones. Can. Soc. Petrol. Geol. Mem., vol. II, pp. 181–190.

Crockett, J.S., Nittrouer, C.A., 2004. The sandy inner shelf as a repository for muddy sediment: an example from Northern California. Cont. Shelf Res. 24, 55–73.

Demirpolat, S., 1991. Surface and near-surface sediments from the continental shelf off the Russian River, northern California. Mar. Geol. 99, 163–173.

Dunbar, G.B., Barrett, P.J., 2005. Estimating palaeobathymetry of wave-graded continental shelves from sediment texture. Sedimentology 1–17.

Edwards, B.D., 2002. Variations in sediment texture on the northern Monterey Bay National Marine Sanctuary continental shelf. Mar. Geol. 181, 83–100.

Eittreim, S.L., Anima, R.J., Stevenson, A.J., Wong, F.L., 2000. Seafloor rocks and sediments of the continental shelf from Monterey Bay to Point Sur, California. USGS Miscellaneous Field Studies Map MF-2345.

Fain, A.M.V., Ogston, A.S., Sternberg, R.W., 2007. Sediment transport event analysis on the western Adriatic continental shelf. Cont. Shelf Res. 27, 431–451.

Fox, J.M., Hill, P.S., Milligan, T.G., Boldrin, A., 2004. Flocculation and sedimentation on the Po River Delta. Mar. Geol. 203, 95–107.

Friedrichs, C.T., Wright, L.D., 2004. Gravity-driven sediment transport on the continental shelf: implications for equilibrium profiles near river mouths. Coast. Eng. 51, 795–811.

Frihy, O.E., Gamai, I.H., 1991. Facies analysis of Nile Delta continental-shelf sediments off Egypt. J. Sea Res. 27 (2), 165–171.

George, D.A., Hill, P.S., Milligan, T.G., 2007. Flocculation, heavy metals (Cu, Pb, Zn) and the sand–mud transition on the Adriatic continental shelf, Italy. Cont. Shelf Res. 27, 475–488.

Goff, J.A., Orange, D.L., Mayer, L.A., Hughes-Clarke, J.E., 1999. Detailed investigation of continental shelf morphology using a high-resolution swath sonar survey; the Eel margin, northern California. Mar. Geol. 154 (1–4), 255–269.

Hill, P.S., Fox, J.M., Crockett, J.S., Curran, K.J., Friedrichs, C.T., Geyer, W.R., Milligan, T.G., Ogston, A.S., Puig, P., Scully, M.E., Traykovski, P.A., Wheatcroft, R.A., 2007. Sediment delivery to the seabed on continental margins. In: Nittrouer, C.A., Austin, J.A., Field, M.E., Kravitz, J.H., Syvitski, J.P.M., Wiberg, P.L. (Eds.), Continental Margin Sedimentation: From Sediment Transport to Sequence Stratigraphy, vol. 37. International Association of Sedimentologists, pp. 49–99. Special Publication Number.

Herbers, T.H.C., Orzech, M., Elgar, S., Guza, R.T., 2003. Shoaling transformation of wave frequency-directional spectra. J. Geophys. Res. 108 (C1), 3013. doi:10.1029/2001JC001304.

Jenkins, C.J., Kettner, A.J., Moore, C., Sharman, G., 2003. goSEABED world seabed data browser. Univ. Colorado, Inst. Arctic and Alpine Res., Boulder, CO, USA. [Web document: "http://instaar.colorado.edu/~jenkinsc/dbseabed/goseabed/interactive/", 6 June 2003].

Liu, J.T., Liu, K., Huang, J.C., 2002. The effect of a submarine canyon on the river sediment dispersal and inner shelf sediment movements in southern Taiwan. Mar. Geol. 181, 357–386.

Liu, J.T., Huang, J.-S., Hsu, R.T., Chyan, J.-M., 2000. The coastal depositional system of a small mountainous river: a perspective from grain-size distributions. Mar. Geol. 165, 63–86.

McCave, I.N., 1972. Transport and escape of fine-grained sediment from shelf areas. In: Swift, D.J.P., Duane, D.B., Pilkey, O.H. (Eds.), Shelf Sediment Transport: Process and Pattern. Dowden, Hutchinson and Ross, New York, pp. 225–247.

Meadows, M.E., Rogers, J., Lee-Thorp, J.A., Bateman, M.D., Dingle, R.V., 2002. Holocene geochronology of a continental-shelf mudbelt off southwestern Africa. Holocene 12 (1), 59–67.

Milligan, T.G., Loring, D.H., 1997. The effect of flocculation on the size distributions of bottom sediment in coastal inlets: implications for metal transport. Water Air Soil Pollut. 99, 33–42.

Milligan, T.G., Hill, P.S., Law, B.A., 2007. Flocculation and the loss of sediment from the Po River plume. Cont. Shelf Res. 27, 309–321.

Milliman, J.D., Syvitski, J.P.M., 1992. Geomorphic/tectonic control of sediment discharge to the ocean: the importance of small mountainous rivers. J. Geol. 100, 525–544.

Milliman, J.D., Rutkowski, C., Meybeck, M., 1995. River Discharge to the Sea, a Global River Index (GLORI). Land-Ocean Interactions in the Coastal Zone (LOICZ), LOICZ Reports and Studies, Netherland Institute for Sea Research, The Netherlands.

Milliman, J.D., Farnsworth, K.L., Albertin, C.S., 1999. Flux and fate of fluvial sediments leaving large islands in the East Indies. Neth. J. Sea Res. 41, 97–107.

Naish, T., Kamp, P.J.J., 1997. Foraminiferal depth paleoecology of Late Pliocene shelf sequences and systems tracts, Wanganui Basin, New Zealand. Sediment. Geol. 110, 237–255.

Palanques, A., Drake, D.E., 1990. Distribution and dispersal of suspended particulate matter on the Ebro continental shelf, northwestern Mediterranean Sea. Mar. Geol. 95, 193–206.

Porter-Smith, R., Harris, P.T., Andersen, O.B., Coleman, R., Greenslade, D., Jenkins, C.J., 2004. Classification of the Australian continental shelf based on predicted sediment threshold exceedance from tidal currents and swell waves. Mar. Geol. 211, 1–20.

Pratson, L.F., Hutton, E.W.H., Kettner, A.J., Syvitski, J.P.M., Hill, P.S., George, D.A., Milligan, T.G., 2007. The impact of floods and storms on the acoustic reflectivity of the inner continental shelf: a modeling assessment. Cont. Shelf Res. 27, 542–559.

Reid, J., Reid, J., Jenkins, C., Zimmermann, M., Williams, S., Field, M., 2006. usSEABED: Pacific Coast (California, Oregon, Washington) Offshore Surficial-sediment Data Release: USGS Data Series 182.

Sanford, L.P., Maa, J.P.Y., 2001. A unified erosion formulation for fine sediments. Mar. Geol. 179, 9–23.

Schiff, K.C., 2000. Sediment chemistry on the mainland shelf of the Southern California Bight. Mar. Pollut. Bull. 40 (3), 268–276.

Short, A.D., Trenaman, N.L., 1992. Wave climate of the Sydney region, an energetic and highly variable ocean wave regime. Aust. J. Mar. Freshw. Res. 43, 765–791.

Snelgrove, P.V.R., Butman, C.A., 1994. Animal sediment relationships revisited — cause versus effect. Oceanogr. Mar. Biol. 32, 111–177.

Stanley, D.J., Addy, S.K., Behrens, E.W., 1983. The mudline: variability of its position relative to shelfbreak. In: Stanley, D.J., Moore, G.T. (Eds.), The Shelfbreak: Critical Interface on Continental Margins. SEPM Special Publication, vol. 33, pp. 279–298. Tulsa, OK.

Storlazzi, C.D., Reid, J.A., Golden, N.E., 2007. Wave-driven spatial and temporal variability in seafloor sediment mobility in the Monterey Bay, Cordell Bank and Gulf of the Farallons National Marine Sanctuaries. U.S. Geological Survey Scientific Investigations Report 2007-5233. 84 pp. http://pubs.usgs.gov/sir/2007/5233/.

Thorton, E.B., Guza, R.T., 1989. Wind wave transformation. In: Seymour, R.J. (Ed.), Nearshore Sediment Transport. Plenum Press, New York, NY, pp. 137–171.

Wiberg, P.L., Drake, D.E., Cacchione, D.A., 1994. Sediment resuspension and bed armoring during high bottom stress events on the northern California inner continental-shelf — measurements and predictions. Cont. Shelf Res. 14, 1191–1219.

Wingfield, D.K., Storlazzi, C.D., 2007. Spatial and temporal variability in oceanographic and meterological forcing along Central California and its implications on nearshore processes. J. Mar. Syst. 68, 457–472.